AIP | Applied Physics Letters

Anomalous enhancement of the thermoelectric figure of merit by V co-doping of Nb-SrTiO3

K. Ozdogan, M. Upadhyay Kahaly, H. N. Alshareef, and U. Schwingenschlögl

Citation: Applied Physics Letters **100**, 193110 (2012); doi: 10.1063/1.4714541
View online: http://dx.doi.org/10.1063/1.4714541
View Table of Contents: http://scitation.aip.org/content/aip/journal/apl/100/19?ver=pdfcov
Published by the AIP Publishing

Anomalous enhancement of the thermoelectric figure of merit by V co-doping of Nb-$SrTiO_3$

K. Ozdogan,[1,2] M. Upadhyay Kahaly,[1] H. N. Alshareef,[1] and U. Schwingenschlögl[1,a)]
[1]*KAUST, Physical Science & Engineering, Thuwal 23955-6900, Kingdom of Saudi Arabia*
[2]*Department of Physics, Yildiz Technical University, 34210 Istanbul, Turkey*

(Received 17 February 2012; accepted 25 April 2012; published online 10 May 2012)

The effect of V co-doping of Nb-$SrTiO_3$ is studied by full-potential density functional theory. We obtain a stronger increase of the carrier density for V than for Nb dopants. While in Nb-$SrTiO_3$ a high carrier density counteracts a high thermoelectric figure of merit, the trend is inverted by V co-doping. The mechanism leading to this behavior is explained in terms of a local spin-polarization introduced by the V ions. Our results indicate that magnetic co-doping can be a prominent tool for improving the thermoelectric figure of merit. © *2012 American Institute of Physics*. [http://dx.doi.org/10.1063/1.4714541]

Multiple technological applications of perovskite oxides have established these systems as prototypical materials with properties such as ferroelectricity, piezoelectricity, colossal magnetoresistance, and many others. Among the perovskite oxides, strontium titanate $SrTiO_3$ (STO) is one of the most popular materials, with a wide gap of about 3.2 eV, and well known for its ferroelectricity. It can be used to construct an efficient non-volatile ferroelectric random access memory.[1,2] It is commonly employed as a standard substrate for growing thin films due to its chemically and compositionally stable structure and small lattice mismatch with many other perovskite oxides.[3–5] Thus, STO-based materials have been investigated intensively in recent years.

Charge carriers can be injected into STO by atom substitution as well as O vacancies and O excess, thereby opening a path to many advanced applications.[6–10] STO can be doped with Nb easily. Its electrical properties transform from an insulator to a conductor with increasing Nb concentration.[11–13] In Nb-doped STO films prepared by pulsed laser deposition, it has been found that the Nb dopants occupy Ti sites and become Nb^{5+} ions, giving away one electron.[11] The electrical conductivity of Nb-doped STO films can be controlled by means of the Nb concentration. Introduction of the high valence cation V^{5+} on the Ti^{4+} sites gives additional control over the electronic response, because such doping suppresses the formation of O vacancies due to the charge neutrality restriction. In addition, V doping leads to injection of excess magnetic moments in the system. Thus, Nb and V co-doped STO films can be employed to generate thermally excited spin currents and a spin-dependent thermoelectric response at the nanoscale.

In the present paper, we therefore study the electronic structures of Nb and V co-doped STO applying first-principles density functional theory. We replace Ti atoms with V and Nb and investigate how the presence of two spin channels affects the transport dependent thermoelectric behavior as compared to merely Nb-doped STO. The chemical similarity of V and Nb seems to indicate that V doping will have the same negative effect on the thermoelectric figure of merit as has been found for an increasing Nb concentration. Therefore, this kind of co-doping has not been explored systematically so far, neither experimentally nor theoretically. However, we will show that V co-doping in fact has an opposite effect and can strongly improve the thermoelectric properties. We elaborate the mechanism leading to this unexpected behavior.

First-principles calculations are carried out with the full-potential linearized augmented plane waves plus local orbitals method as implemented in the WIEN2K code,[14] within the framework of density functional theory. We study two Nb and V dopant concentrations of $x = 12.5\%$ and 25% in $SrTi_{1-2x}Nb_xV_xO_3$ employing the supercell approach.[15–18] For $x = 12.5\%$, we address three different configurations with varying Nb-V distance, whereas for $x = 25\%$ we investigate one configuration. A $2 \times 2 \times 6$ supercell of the primitive cubic unit cell with totally 120 atoms in total is employed, where 4 STO layers are considered to be the substrate. See the cross-sections of the structures shown in Fig. 1 for a definition of the different systems under investigation.

The Brillouin zone is sampled using a Monkhorst-Pack $6 \times 6 \times 2$ k-space grid and the exchange-correlation potential is treated in the generalized gradient approximation.[19] For the wave function expansion inside the atomic spheres, we select a maximum value of $\ell_{max} = 12$ and employ a plane-wave cutoff of $R_{mt}K_{max} = 6$ with $G_{max} = 24$. The valence orbitals comprise the Sr 4s, 5s, and 4p states, Ti 4s, 3p, and 3d states, Nb 5s, 4p, and 4d states, V 4s, 3p, and 3d states, and O 2s and 2p states. All lower states are treated as semi-core and core states. The muffin-tin sphere radii (in atomic units) are set to 2.5 for Sr, 1.9 for Ti, 1.8 for Nb and V, and 1.6 for O. All calculation parameters have been checked carefully for convergence to obtain correct results. To capture the effects of structural relaxation on the local chemical bonding and physical properties, the atomic forces in the supercell have been converged down to less than 7 mRy/Bohr. We use the experimental lattice constant of $SrTiO_3$ ($a = 3.905$ Å) for the whole supercell. For predicting the Seebeck coefficient, we employ the BoltzTraP code,[20] which is interfaced with WIEN2K. This code is based on Boltzmann theory and calculates band structure dependent quantities such as the electrical and thermal conductivities within the rigid band approach. For calculating the transport

a)Electronic mail: udo.schwingenschlogl@kaust.edu.sa.

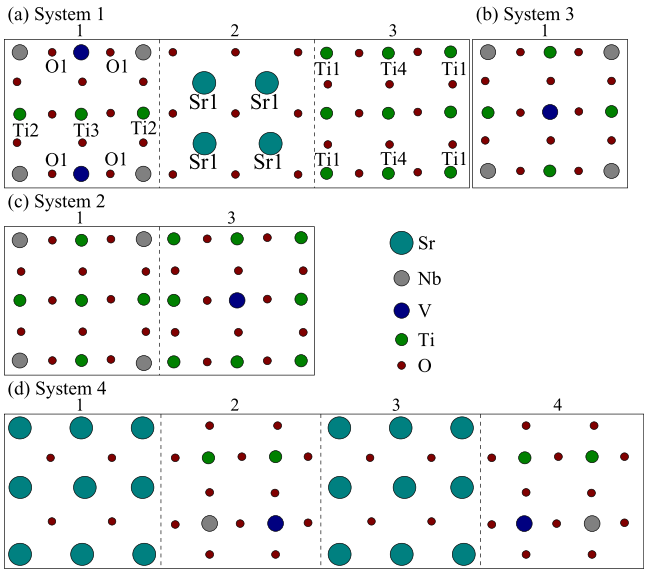

FIG. 1. Cross-sections of Nb and V co-doped STO/$SrTi_{1-2x}Nb_xV_xO_3$/STO ($x = 12.5\%$, 25%). (a) Minimum energy configuration for $x = 12.5\%$. The three columns are three adjacent layers, with Nb and V atoms doped in layer 1. The atoms marked with indices are addressed in Fig. 3. (b) Layer 1 of the second lowest energy configuration (system 3). Layers 2 and 3 are identical to (a). (c) Layers 1 and 3 of the third lowest energy configuration (system 2) for $x = 12.5\%$. Layer 2 is identical to (a). (d) Four adjacent layers for $x = 25\%$.

coefficients, we use a very fine k-space grid with 3872 (4060) k-points for systems 1 and 4 (systems 2 and 3).

Our calculations show that clustering of the Nb and V dopants is energetically favorable. While an Nb-V distance of 3.905 Å (system 1) leads to the minimum energy configuration, distances of 5.522 Å (system 2) and 6.717 Å (system 3) result in energy costs of 17 and 72 meV, respectively. The electronic effect of Nb and V co-doping on STO is demonstrated by the density of states (DOS) of the $SrTi_{1-2x}Nb_xV_xO_3$ heterostructure in Fig. 2. While the total DOS of the doped system remains essentially the same irrespective of the dopant positions (systems 1, 2, and 3), an increase in the concentration enhances the DOS at the Fermi energy (system 4). Since the STO band structure remains mainly intact with new contributions from the V and Nb dopants, we expect an enhancement

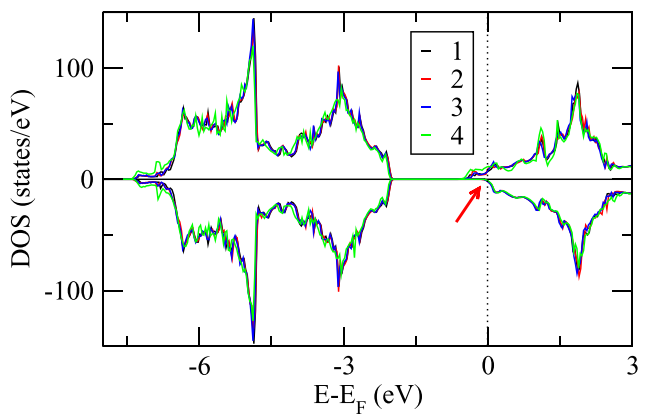

FIG. 2. Total DOS of the STO/$SrTi_{1-2x}Nb_xV_xO_3$/STO heterostructure. Systems 1, 2, and 3 ($x = 12.5\%$) contain 1 Nb atom and 1 V atom, while system 4 ($x = 25\%$) contains 2 Nb and 2 V atoms. The arrow highlights the main contribution to the polarization.

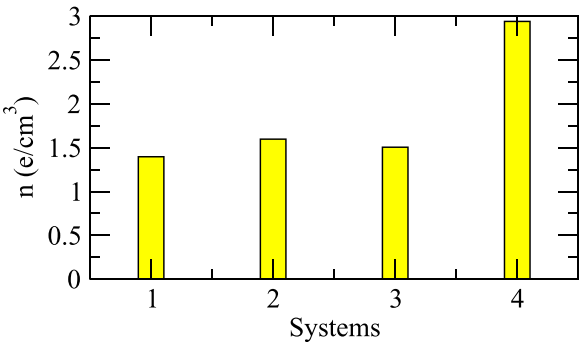

FIG. 3. Carrier densities of the systems under investigation.

of the overall carrier density. The intrinsic carrier density at zero Kelvin is given by $n_0 = \int_{E_c}^{E_F} DOS(E)dE$, where E_c is the bottom of the conduction band, and is observed to be directly proportional to the amount of Nb and V doping, see Fig. 3. For $x = 12.5\%$, we note a slight dependence on the specific Nb and V positions. Due to a finite interaction with the Nb and V dopants, a slight hybridization is found for the Sr states, see, for example, the DOS of the Sr1 atom (closest to the V dopant) in Fig. 4. The partial Ti and O DOSs are modified in the presence of Nb and V dopants more significantly, see Fig. 4. Note that the effect of the V dopants on the partial DOS of neighboring atoms is much more prominent than that of Nb, because of the additional d states of V and its higher electronegativity. The V ion displays a large DOS at the Fermi energy, while the Nb DOS is much smaller.

In the minority spin channel, the Fermi energy lies near the conduction band edge. The main contributions to the top of the valence band are due to the O 2p states, with some admixtures from the Ti 3d, V 3d, and Nb 4d states. The main contributions to the bottom of the conduction band originate

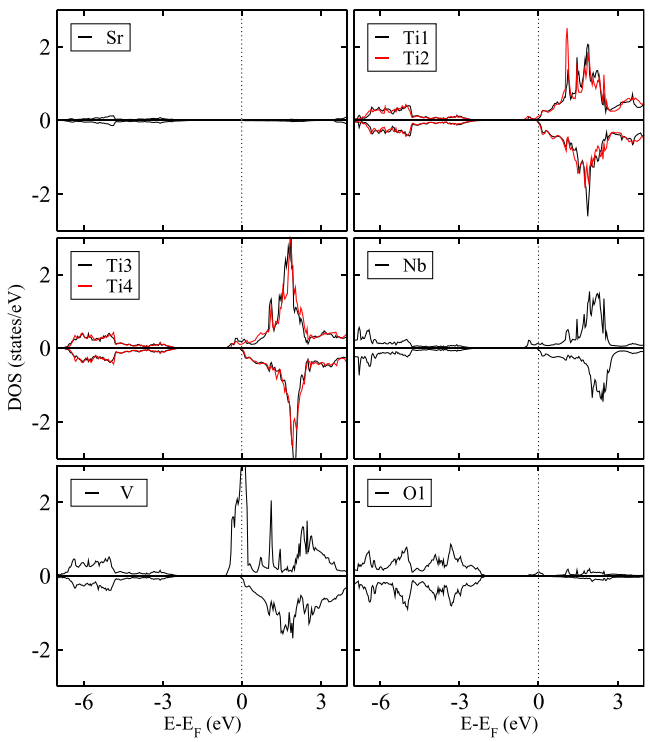

FIG. 4. Partial DOS of the STO/$SrTi_{1-2x}Nb_xV_xO_3$/STO heterostructure for $x = 12.5\%$.

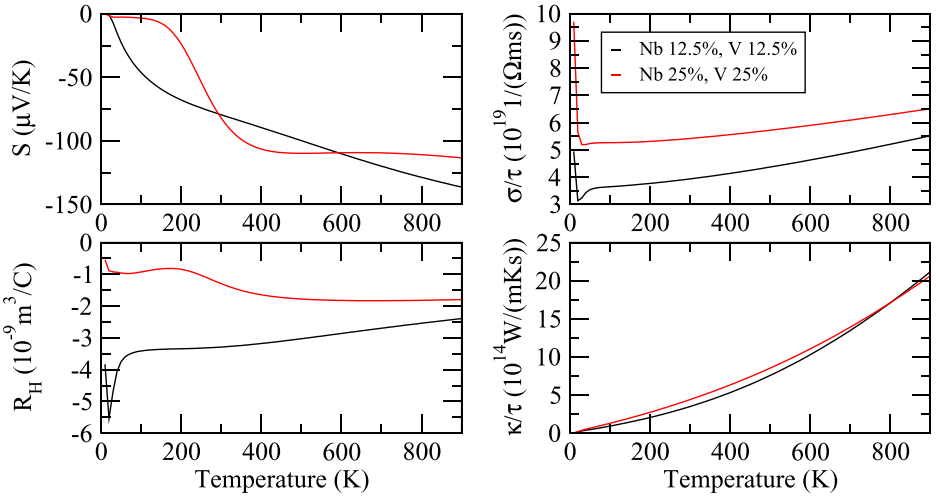

FIG. 5. Comparison of the thermoelectric properties of systems 1 ($x = 12.5\%$) and 4 ($x = 25\%$).

from the V 3*d* states with admixtures from the Nb 4*d*, Ti 3*d*, and (slightly) O 2*p* states. The majority spin channel exhibits itinerant *d* states of V and Nb across the Fermi energy, with a major contribution to the conduction band. When we increase the Nb and V concentrations, the gross shape of the DOS remains similar, but it shifts to lower energy (see Fig. 2), because the number of conduction electrons induced by the Nb and V dopants increases. For a decreasing distance between Ti and the V dopant (atoms Ti3 and Ti4, for example), the DOS at the Fermi energy grows. Due to hybridization with mainly V states (partially with Nb), the 2*p* states of neighboring O atoms contribute slightly at the Fermi energy. In addition, for $x = 0.125$, the shape of the O 2*p* DOS shows some changes, especially in the valence band, depending on the O-V and O-Nb distances. A strong hybridization is observed between the O atoms and neighbouring V and Nb atoms. Interestingly, also the V, Nb, and Ti states show signs of interaction. The Sr DOS hardly changes with the Nb-Sr distance. A metallic nature of STO films doped with Nb and V for concentrations of 12.5% and 25% is clearly reflected by Figs. 2 and 4.

Let us next elaborate the effect of the V and Nb doping on the thermoelectric properties of STO. Because the thermoelectric figure of merit (Z) fulfills $Z = S^2\sigma/\kappa \propto 1/n$, an increased carrier density n in Nb-STO results in a reduction of Z. As n also increases for V doping, see above, naively the same effect would be expected in this case. However, our calculations establish exactly the opposite trend. To be more specific, we employ Boltzmann transport theory together with the rigid band approach. This approach is expected to yield very good estimates for the thermoelectric transport tensors (the electrical and thermal conductivities) and Seebeck coefficient.[19–22] A comparison of the Seebeck coefficient, electrical conductivity, Hall coefficient, and the electronic part of the thermal conductivity as a function of the temperature is shown in Fig. 5 for systems 1 and 4. Assuming that the relaxation time τ is not direction dependent, we find that the Seebeck coefficient S decreases with the temperature. While for $x = 25\%$, a critical temperature of $T_c \sim 400$ K is found above which $S(T)$ is virtually constant, this temperature is shifted to $T_c \sim 1000$ K for the lower Nb and V doping of $x = 12.5\%$. Flat areas in $S(T)$ reflect a linear temperature dependence of the thermovoltage. Consistent with the trend of the carrier density, the electrical conductivity σ in Fig. 5(b) is also found to be directly proportional to the dopant concentration. However, the electronic thermal conductivity κ in Fig. 5(d) is almost doping independent, thereby making the denominator of Z a constant. The Hall coefficient R_H demonstrates an ambipolar transport. While both electrons and holes are important, the electron mobility still is higher. The enhanced negative value of R_H for $x = 25\%$, see Fig. 5(c), suggests that the extra *d* electrons from the increased doping contribute strongly to the transport.

While the contribution of the minority spin states to S (and thus Z) changes only little with the temperature, see Fig. 6, filling of the majority bands with increasing temperature prominently alters S and Z for varying Nb and V concentrations. We highlight the effect of the V doping on the thermoelectric response in Fig. 7. While an increased concentration of Nb reduces Z, V co-doping results in a substantial increase of Z. The maximum value is found for

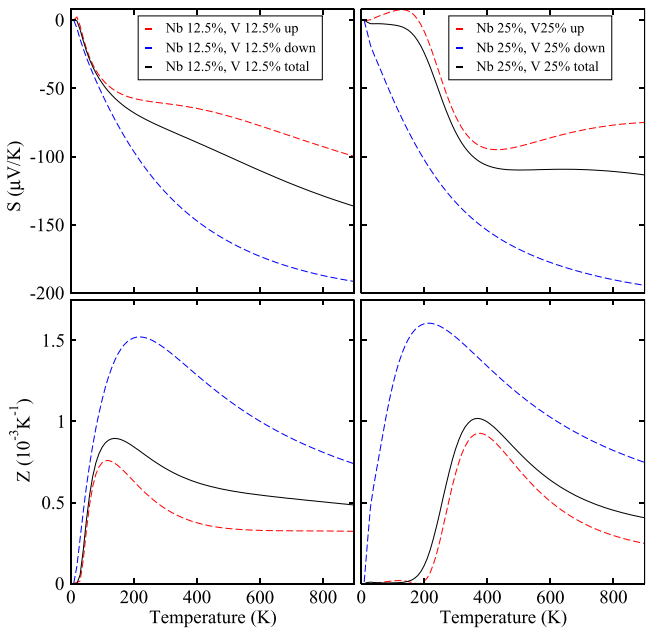

FIG. 6. Spin dependent Seebeck coefficient and thermoelectric figure of merit for systems 1 ($x = 12.5\%$) and 4 ($x = 25\%$).

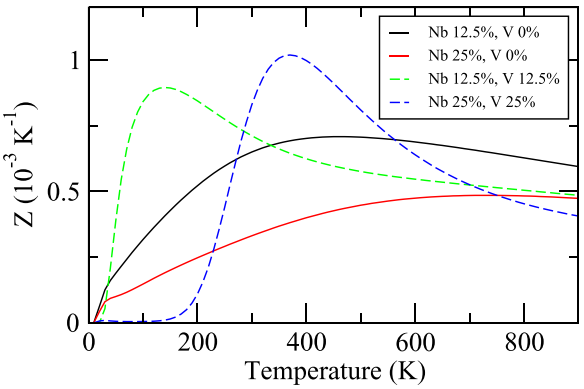

FIG. 7. Variation of the thermoelectric figure of merit with the doping.

$SrTi_{0.5}Nb_{0.25}V_{0.25}O_3$, amounting to $1.1 \cdot 10^{-3}$ K^{-1} at 400 K. The enhancement of Z by V co-doping (while further Nb doping results in a reduction) can be explained by the spin polarization introduced by the V ions. Figure 2 shows around E_F a substantial number of spin majority states but only a tiny number of spin minority states. For this reason, the spin majority and minority states have little interaction and almost behave as independent species. Since the spin majority carrier density is large, the contribution of these states to Z is small, see the red dashed curve in Fig. 6. On the other hand, the small population of spin minority states (Fig. 2) results in a high value of Z, see the blue dashed curve in Fig. 6. As a consequence, the cumulative figure of merit is enhanced under V co-doping due to the magnetic nature of the V ions when substituted in STO.

In conclusion, we have investigated the electronic structure as well as the transport and thermoelectric behavior of V co-doped Nb-STO. We find a nearly monotonous increase of the carrier density with the Nb and V concentrations. A linear temperature dependence of the thermovoltage above T_c makes the system a very promising candidate for thermoelectric devices. Contradicting the naive expectation, V co-doping of Nb-STO turns out to improve the thermoelectric figure of merit. If the V concentration is increased from 12.5% to 25%, for example, a substantial enhancement of 28% is found at 370 K. The anomalous behavior is attributed to a splitting of the mobile electrons in the vicinity of the Fermi energy into two largely decoupled spin channels. While the spin majority channel constitutes the main part of the carrier density, the spin minority channel enhances the thermoelectric figure of merit. Magnetic co-doping in this sense can be a highly efficient mechanism for improving the thermoelectric properties.

[1]P. W. Peacock and J. Robertson, Appl. Phys. Lett. **83**, 5497 (2003).
[2]V. Thavasi, V. Renugopalakrishnan, R. Jose, and S. Ramakrishna, Mater. Sci. Eng. R **63**, 81 (2009).
[3]J. Javier and G. Philippe, Nature **422**, 506 (2003).
[4]B. H. Lu, S. Y. Dai, Z. H. Chen, L. Yan, Y. L. Zhou, and G. Z. Yang, Chin. Sci. Bull. **48**, 1328 (2003).
[5]M. Kubo, Y. Oumi, R. Miura, A. Stirling, and A. Miyamoto, Phys. Rev. B **56**, 13535 (1997).
[6]Y. Watanebe, J. G. Bednorz, A. Bietsch, C. Gerber, D. Widmer, A. Beck, and S. J. Wind, Appl. Phys. Lett. **78**, 3738 (2001).
[7]J. Inaba and T. Katsufuji, Phys. Rev. B **72**, 054208 (2005).
[8]T. Hara, Mater. Chem. Phys. **91**, 243 (2005).
[9]T. H. Fang, Y. J. Hsiao, Y. S. Chang, and Y. H. Chang, Mater. Chem. Phys. **100**, 418 (2006).
[10]A. Tkach, P. M. Vilarinho, A. L. Kholkin, A. Paskhin, S. Veljko, and J. Petzelt, Phys. Rev. B **73**, 104113 (2006).
[11]T. Tomio, H. Miki, H. Tabata, T. Kawai, and S. Kawai, J. Appl. Phys. **76**, 5886 (1994).
[12]S. Ohta, T. Nomura, H. Ohta, M. Hirano, H. Hosono, and K. Koumoto, Appl. Phys. Lett. **87**, 092108 (2005).
[13]Y. Ishida, R. Eguchi, M. Matsunami, K. Horiba, M. Taguchi, A. Chainani, Y. Senba, H. Ohashi, H. Ohta, and S. Shin, Phys. Rev. Lett. **100**, 056401 (2008).
[14]P. Blaha, K. Schwarz, G. Madsen, D. Kvasicka, and J. Luitz, WIEN2K, *An Augmented Plane Wave + Local Orbitals Program for Calculating Crystal Properties* (Technical University of Vienna, Vienna, 2001).
[15]S. Nazir and U. Schwingenschlögl, Appl. Phys. Lett. **99**, 073102 (2011).
[16]M. Upadhyay Kahaly, S. Nazir, and U. Schwingenschlögl, Appl. Phys. Lett. **99**, 123501 (2011).
[17]U. Schwingenschlögl and C. Schuster, EPL **86**, 27005 (2009).
[18]U. Schwingenschlögl and C. Schuster, Phys. Rev. Lett. **102**, 227002 (2009).
[19]K. Ozdogan, M. Upadhyay Kahaly, S. R. Sarath Kumar, H. N. Alshareef, and U. Schwingenschlögl, J. Appl. Phys. **111**, 054313 (2012).
[20]G. K. H. Madsen and D. J. Singh, Comput. Phys. Commun. **175**, 67 (2006).
[21]X. G. Guo, X. S. Chen, and W. Lu, Solid State Commun. **126**, 441 (2003).
[22]Y. I. Ravich, B. A. Efimova, and I. A. Smirov, *Semiconducting Lead Chalcogenides* (Plenum, New York, 1970).